NEWTONIAN HEATING EFFECT ON HEAT ABSORBING UNSTEADY MHD RADIATING AND CHEMICALLY REACTING FREE CONVECTION FLOW PAST AN OSCILLATING VERTICAL POROUS PLATE

B. PRABHAKAR REDDY*
Department of Mathematics and Statistics
College of Natural and Mathematical Sciences
The University of Dodoma, P. Box 338 Dodoma, TANZANIA
E-mail: prabhakar.bijjula@gmail.com

O. D. MAKINDE
Faculty of Military Science, Stellenbosch University
Private Bag X2, Saldanha 7395, SOUTH AFRICA

In this article, we have discussed in detail the effect of Newtonian heating on MHD unsteady free convection boundary layer flow past an oscillating vertical porous plate embedded in a porous medium with thermal radiation, chemical reaction and heat absorption. The governing PDEs of the model together with related initial and boundary conditions have been solved numerically by the finite element method. The dimensionless velocity, temperature and concentration profiles are analyzed graphically due to the effects of key parameters in the concerned model problem. Computed results for the skin friction coefficient, Nusselt number and Sherwood number are put in tabular form. It is observed that the thermal and mass buoyancy effects support the velocity whilst a reverse effect is noticed when the strength of the magnetic field is increased. The velocity and temperature enhances with an increase in the Newtonian heating and thermal radiation whilst a reverse effect is observed with an increase in the Prandtl number and heat absorption parameter. Increasing Schmidt number and chemical reaction parameter tends to depreciate both velocity and concentration. The Newtonian heating, thermal radiation and magnetic field tends to decrease in the skin friction. The Nusselt number increases with increasing Newtonian heating and heat absorption parameters. An increase in the Schmidt number and chemical reaction rate tends to improve the Sherwood number.

Key words: Newtonian heating, radiation parameter, chemical reaction rate, oscillating plate, heat absorption parameter.

1. Introduction

The problem of convective flow with heat and mass transfer in the presence of a chemical reaction has received substantial amount of concern in recent years due to its wide range of practical applications in many areas of science and engineering. In many chemical engineering processes, a chemical reaction occurs between a foreign mass and the fluid in which the plate is moving. These processes take place in numerous industrial applications such as manufacturing of ceramics or glassware, polymer production and food processing. Chemical reaction can be classified as either homogeneous or heterogeneous processes, which depends on whether they occur at an interface or as a single phase volume reaction. Many transport processes exist in mass transfer in nature as a result of combined buoyancy effects of thermal diffusion and diffusion of chemical species. Das *et al.* [1] studied the effect of homogeneous first order chemical reaction on the flow past an impulsively started infinite vertical plate with uniform heat flux and mass transfer. Muthucumaraswamy and Ganesan [2] discussed the effect of chemical reaction on an unsteady flow past an impulsively started vertical plate which is subjected to uniform mass flux and in the presence of heat

---

* To whom correspondence should be addressed

transfer. Raptis and Perdikis [3] studied numerically the steady two dimensional flow of an incompressible viscous and electrically conducting fluid over a non-linear semi-infinite stretching sheet in the presence of chemical reaction under the influence of a magnetic field. Cortell [4] studied MHD flow and mass transfer of an electrically conducting fluid of second grade over a nonlinear stretching sheet with chemically reactive species in a porous medium. Mass transfer effects on an isothermal vertical oscillating plate in the presence of chemical reaction were analyzed by Muthucumaraswamy and Janakiraman [5]. Mahapatra *et al.* [6] studied the effects of chemical reaction on a free convection flow through a porous medium bounded by a vertical surface. Rajesh and Varma [7] investigated the impact of chemical reaction on a free convection flow past an exponentially accelerated vertical plate. MHD and chemical reaction effects on a free convection flow with variable temperature and mass diffusion were discussed by Rajesh [8]. El-Fayez [9] analyzed chemical reaction effect on an unsteady free convection flow past an infinite vertical permeable moving plate with variable temperature. Sehkar and Reddy [10] studied the effects of chemical reaction on MHD free convective oscillatory flow past a porous plate with viscous dissipation and heat sink.

In most of the above cited research studies, the effects of thermal radiation on the flow are not taken into account. However, the problem of MHD free convection heat and mass diffusion in the presence of thermal radiation play a vital role in manufacturing processes such as glass production, design of fins, steel tolling, furnace design, casting and levitation, etc. Moreover, several engineering processes occur at high temperature where the knowledge of radiative heat transfer becomes crucial for the design of pertinent equipment, nuclear power plants, gas turbines and various propulsion devices for aircraft, missiles, satellites, and space vehicles are examples of such engineering areas. Soundalgekhar and Takhar [11] analyzed the radiation effects on a free convection flow past a semi-infinite vertical plate. Takhar *et al.* [12] studied the effect of radiation on MHD free convection flow of a radiating gas past a semi-infinite vertical plate. Radiation effects on free convection flow past a moving plate was discussed analytically by Raptis and Perdikis [13]. Chamkha *et al.* [14] studied a radiative free convective non-Newtonian fluid flow past a wedge embedded in a porous medium. Muthucumaraswamy and Janakiraman [15] analyzed MHD and radiation effects on a moving isothermal vertical plate with variable mass diffusion. Rajesh and Varma [16] investigated the radiation effects on MHD flow through a porous medium with variable temperature and mass diffusion. Effects of thermal radiation on a transient MHD free convection flow over a vertical surface embedded in a porous medium with periodic boundary conditions were investigated by Mebine and Adigio [17]. Sharma and Deka [18] analyzed thermal radiation and oscillating temperature effects on an unsteady MHD flow past a semi infinite vertical porous plate in the presence of chemical reaction. Muralidhran and Muthucumaraswamy [19] discussed the radiation effects on a linearly accelerated plate with variable mass diffusion in the presence of a magnetic field.

Convection flows with combined heat and mass transfer past a vertical plate are usually modeled by considering variable surface temperature or ramped wall temperature or constant heat flux. Though, in many practical applications where the heat transfer from the surface is proportional to the local surface temperature known as the Newtonian heating effect, when the above conditions fail to work Newtonian heating conditions are highly needed. The applications of Newtonian heating are found significant engineering applications such as heat exchangers, turbines and also in convective flows set up when the bounding surface absorbs heat by solar radiation. The natural convection boundary layer flow over a vertical surface with Newtonian heating was first studied by Merkin [20]. Lesnic *et al.* [21, 22] studied free convection boundary layer flows along vertical and horizontal surfaces in a porous medium generated by Newtonian heating. Subsequently, a free convection boundary layer flow above a nearly horizontal surface in a porous medium with Newtonian heating was reported by Lesnic *et al.* [23]. An unsteady free convection flow past an impulsively started vertical plate with Newtonian heating was studied by Chaudhary and Jain [24]. Salleh *et al.* [25] studied a forced convection boundary layer flow at a forward stagnation point with Newtonian heating. A steady boundary layer flow over a stretching sheet with Newtonian heating was studied by Salleh *et al.* [26]. Abid *et al.* [27] studied heat and mass transfer past an oscillating vertical plate with Newtonian heating where the governing equations of the problem were solved by the Laplace transform technique. Subsequently, Abid *et al.* [28] studied an unsteady boundary layer MHD free convection flow in a porous medium with constant mass diffusion and Newtonian heating analytically by the

Laplace transform technique. An unsteady hydro-magnetic natural convection flow past an impulsively moving vertical plate with Newtonian heating in a rotating system was studied by Seth *et al.* [29].

The above comprehensive review of literature demonstrates that the problem of the Newtonian heating effect on an MHD unsteady free convective boundary layer flow past an oscillating vertical plate in the presence of thermal radiation, chemical reaction and heat absorption has not been studied. Such a model problem finds ample engineering and industrial applications such as manufacturing of ceramics or glassware, polymer production and food processing, heat exchangers, design of fins, steel tolling, furnace design, casting and levitation, design of pertinent equipment, nuclear power plants and gas turbines, etc. The main purpose of this problem is to fill this gap. The dominant finite element method has been employed to solve the governing system of PDEs. The behavior of the velocity, temperature, concentration, skin friction, Nusselt number and Sherwood number are discussed under the influence of various embedded parameters through graphs and tables.

2. Mathematical model

Consider an unsteady magneto-hydrodynamic (MHD) free convective boundary layer flow of a viscous incompressible electrically conducting radiating and reacting fluid past an oscillating infinite vertical porous plate embedded in a porous medium. The $x'-$ axis is measured along the plate in the vertically upward direction and the $y'-$ axis measured normal to it. A uniform magnetic field of strength B_0 is applied in the direction perpendicular to the flow. The magnetic Reynolds number is assumed to be very small so that the induced magnetic field is negligible. The plate is infinite in the $x'-$ direction, so all the field quantities become functions of the space coordinate y' and time t'. Initially, the plate and fluid are at rest with constant temperature T'_∞ and concentration C'_∞. At time $t' > 0$, the plate starts an oscillatory motion in its own plane with the velocity $U_0 \cos(\omega' t')$ against the gravitational field, where U_0 is the amplitude of the plate oscillations and ω' is the frequency of oscillations. Simultaneously, heat transfer from the plate to the fluid is proportional to the local surface temperature T' and the concentration near the plate is raised from C'_∞ to C'_w. Coupled the above assumptions with the usual Boussinesq's approximation, the following governing PDEs of the model are derived as:

$$\frac{\partial u'}{\partial t'} = v\frac{\partial^2 u'}{\partial y'^2} - \frac{\sigma B_0^2}{\rho}u' - \frac{v\varphi}{K'}u' + g\beta(T'-T'_\infty) + g\beta^*(C'-C'_\infty), \tag{2.1}$$

$$\rho C_p \frac{\partial T'}{\partial t'} = k\frac{\partial^2 T'}{\partial y'^2} - \frac{\partial q_r}{\partial y'} - Q'_0(T'-T'_\infty), \tag{2.2}$$

$$\frac{\partial C'}{\partial t'} = D\frac{\partial^2 C'}{\partial y'^2} - k_r'(C'-C'_\infty). \tag{2.3}$$

The associated initial and boundary conditions are:

$$t' \le 0; \quad u' = 0, \quad T' = T'_\infty, \quad C' = C'_\infty \quad \text{for all} \quad y' \ge 0, \tag{2.4}$$

$$t' > 0; \quad u' = U_0\cos(\omega' t'), \quad \frac{\partial T'}{\partial y'} = -h_s T', \quad C' = C'_w, \quad \text{at} \quad y' = 0, \tag{2.5}$$

$$u' \to 0, \quad T' \to T'_\infty, \quad C' \to C'_\infty, \quad \text{as} \quad y' \to \infty. \tag{2.6}$$

The radiation heat flux under the Rosseland approximation Magyari and Pantokratoras [30] is expressed by

$$q_r = -\frac{4\sigma^\bullet}{3k^*}\frac{\partial T'^4}{\partial y'} \tag{2.7}$$

where $\sigma^\bullet$ is the Stefan-Boltzmann constant and k^* is the mean absorption coefficient. It is assumed that the temperature differences within the flow are sufficiently small such that T'^4 is expressed as the linear function of temperature. Thus expanding T'^4 about T'_∞ using the Taylor series expansion and neglecting second and higher order terms; we obtain

$$T'^4 \cong T'^4_\infty + 4T'^3_\infty(T'-T'_\infty) \cong 4T'^3_\infty T' - 3T'^4_\infty . \tag{2.8}$$

In view of Eqs.(2.7) and (2.8), Eq.(2.2) reduces to the following form:

$$\rho C_p \frac{\partial T'}{\partial t'} = k\left(1 + \frac{16\sigma^\bullet T'^3_\infty}{3kk^*}\right)\frac{\partial^2 T'}{\partial y'^2} - Q'_0(T'-T'_\infty) . \tag{2.9}$$

Introducing the following dimensionless parameters and quantities;

$$u = \frac{u'}{U_0}, \quad \eta = \frac{y'U_0}{v}, \quad t = \frac{t'U_0^2}{v}, \quad \omega = \frac{\omega'v}{U_0^2}, \quad S_c = \frac{v}{D}, \quad P_r = \frac{\mu C_p}{k},$$

$$k_r = \frac{k'_r v}{U_0^2}, \quad \frac{1}{K} = \frac{v^2\varphi}{K'U_0^2}, \quad R = \frac{16\sigma^\bullet T'^3_\infty}{3kk^*}, \quad Q_H = \frac{Q_0 v}{\rho U_0^2}, \quad \theta = \frac{(T'-T'_\infty)}{T'_\infty},$$

$$M^2 = \frac{\sigma B_0^2 v}{\rho U_0^2}, \quad \phi = \frac{(C'-C'_\infty)}{(C'_w-C'_\infty)}, \quad G_r = \frac{g\beta v T'_\infty}{U_0^3}, \quad G_m = \frac{g\beta v(C'-C'_\infty)}{U_0^3},$$

into Eqs.(2.1), (2.3) and (2.9), the following dimensionless governing system of PDEs are obtained:

$$\frac{\partial u}{\partial t} = \frac{\partial^2 u}{\partial \eta^2} - M^2 u - \frac{1}{K}u + G_r\theta + G_m\phi , \tag{2.10}$$

$$\frac{\partial \theta}{\partial t} = \frac{(1+R)}{P_r}\frac{\partial^2 \theta}{\partial \eta^2} - Q_H\theta , \tag{2.11}$$

$$\frac{\partial \phi}{\partial t} = \frac{1}{S_c}\frac{\partial^2 \phi}{\partial \eta^2} - k_r\phi . \tag{2.12}$$

The initial and boundary conditions in dimensionless form become:

$$t \leq 0; u = 0, \quad \theta = 0, \quad \phi = 0, \quad \text{for all} \quad \eta \geq 0, \tag{2.13}$$

$$t > 0;\ u = \cos(\omega t),\quad \frac{\partial\theta}{\partial\eta} = -\gamma(1+\theta),\quad \phi = 1,\ \text{at}\ \ \eta = 0\,, \tag{2.14}$$

$$u \to 0,\quad \theta \to 0,\quad \phi \to 0,\quad \text{as}\quad \eta \to \infty\,. \tag{2.15}$$

Here $\gamma = h_s \nu / U_0$ is the Newtonian heating parameter. It is importance to note that Eq.(2.14) gives $\theta = 0$, when $\gamma = 0$, corresponding to $h_s = 0$ and consequently, no heating exists from the plate (Salleh *et al.* [26] and Abid *et al.* [27]).

3. Solution of the problem by FEM

The dimensionless governing system of coupled PDEs (2.10)-(2.12) with related initial and boundary conditions (2.13)-(2.15) have been solved numerically for various values of involved parameters by employing the finite element method. The finite element method is a numerical and computer based method employ to solve many engineering problems, which occur in different fields such as fluid mechanics, heat transfer, electrical systems, solid mechanics and chemical engineering, etc. A detailed discussion of the numerical procedure was given in Reddy [31] and Bathe [32].

Variational formulation

The variational form associated with Eqs.(2.10)-(2.12) over the typical two-nodded linear element (η_e, η_{e+1}) is given by:

$$\int_{\eta_e}^{\eta_{e+1}} w_1 \left[\left(\frac{\partial u}{\partial t}\right) - \left(\frac{\partial^2 u}{\partial \eta^2}\right) + M^2 u + \frac{1}{K} u - (G_r \theta + G_m \phi) \right] d\eta = 0\,, \tag{3.1}$$

$$\int_{\eta_e}^{\eta_{e+1}} w_2 \left[\left(\frac{\partial\theta}{\partial t}\right) - \frac{(1+R)}{P_r}\left(\frac{\partial^2\theta}{\partial\eta^2}\right) + Q_H \theta \right] d\eta = 0\,, \tag{3.2}$$

$$\int_{\eta_e}^{\eta_{e+1}} w_3 \left[\left(\frac{\partial\phi}{\partial t}\right) - \frac{1}{S_c}\left(\frac{\partial^2\phi}{\partial\eta^2}\right) + k_r \phi \right] d\eta = 0 \tag{3.3}$$

where w_1, w_2 and w_3 are weight functions and may be viewed as the variations in u, θ and ϕ, respectively. Upon application of integration by parts to reduce order of spatial derivatives which allows the application of initial and boundary conditions, the following equations are obtained:

$$\int_{\eta_e}^{\eta_{e+1}} \left[\begin{array}{c} \left(\frac{\partial w_1}{\partial\eta}\right)\left(\frac{\partial u}{\partial\eta}\right) + w_1\left(\frac{\partial u}{\partial t}\right) + \left(M^2 u\right) w_1 + \left(\frac{1}{K}u\right) w_1 \\ -(G_r\theta + G_m\phi) w_1 \end{array} \right] d\eta - \left[w_1\left(\frac{\partial u}{\partial\eta}\right) \right]_{\eta_e}^{\eta_{e+1}} = 0\,, \tag{3.4}$$

$$\int_{\eta_e}^{\eta_{e+1}} \left[\frac{(1+R)}{P_r}\left(\frac{\partial w_2}{\partial\eta}\right)\left(\frac{\partial\theta}{\partial\eta}\right) + w_2\left(\frac{\partial\theta}{\partial t}\right) + (Q_H\theta) w_2 \right] d\eta - \frac{(1+R)}{P_r}\left[w_2\left(\frac{\partial\theta}{\partial\eta}\right) \right]_{\eta_e}^{\eta_{e+1}} = 0\,, \tag{3.5}$$

$$\int_{\eta_e}^{\eta_{e+1}} \left[\frac{1}{S_c} \left(\frac{\partial w_3}{\partial \eta} \right) \left(\frac{\partial \phi}{\partial \eta} \right) + w_3 \left(\frac{\partial \phi}{\partial t} \right) + (k_r \phi) w_3 \right] d\eta - \frac{1}{S_c} \left[w_3 \left(\frac{\partial \phi}{\partial \eta} \right) \right]_{\eta_e}^{\eta_{e+1}} = 0 . \tag{3.6}$$

Finite element formulation

The finite element model may be obtained from Eqs.(3.4)-(3.6) by substituting appropriate finite element approximations of the form:

$$u = \sum_{j=1}^{2} u_j^e \psi_j^e, \quad \theta = \sum_{j=1}^{2} \theta_j^e \psi_j^e, \quad \phi = \sum_{j=1}^{2} \phi_j^e \psi_j^e, \tag{3.7}$$

with

$$w_1 = w_2 = w_3 = \psi_j^e \left(j = 1, 2 \right)$$

where u_j^e, θ_j^e and ϕ_j^e are respectively, velocity, temperature and concentration of the fluid at the jth node of the eth element $\left(\eta_e, \eta_{e+1} \right)$ and ψ_j^e's are the shape functions over the typical element $\left(\eta_e, \eta_{e+1} \right)$ and are taken as:

$$\psi_1^e = \frac{\eta_{e+1} - \eta}{\eta_{e+1} - \eta_e}, \quad \psi_2^e = \frac{\eta - \eta_e}{\eta_{e+1} - \eta_e} \quad \text{where} \quad \left(\eta_e \le \eta \le \eta_{e+1} \right). \tag{3.8}$$

The whole domain is divided into a set of *80* line elements of equal width *0.05*, each element being two nodded. Each element matrix is of order *10×10*. The boundary condition $\eta = \infty$ has been fixed as *4*, which lies very well outside the momentum, energy and concentration boundary layers. Using Eqs. (3.7) and (3.8) into Eqs. (3.4)-(3.6) after assembly of all the element equations by inter-element connectivity conditions, we obtain a matrix of order *324×324*. The obtained system of equations is non-linear therefore an iterative scheme has been used to solve it. The system is linearized by incorporating known function. After imposing the boundary conditions (2.13)-(2.15) only a system of *317* equations remains and these equations have been solved by using the Gauss elimination method by maintaining the desired accuracy *0.0005*.

The skin friction, rate of heat and mass transfer in terms of Nusselt and Sherwood numbers at the plate are given by

$$\tau = - \left(\frac{\partial u}{\partial \eta} \right)_{\eta=0}, \quad N_u = - \left(\frac{\partial \theta}{\partial \eta} \right)_{\eta=0} \text{ and } S_h = - \left(\frac{\partial \phi}{\partial \eta} \right)_{\eta=0} .$$

Validation of numerical procedure

In order to validate the present numerical procedure, a comparison has been made of the computed Nusselt number N_u in the absence of the heat absorption parameter $(Q_H = 0)$ and the Sherwood number S_h in the absence of the chemical reaction rate $(k_r = 0)$ numerically by the finite element method and those of Abid *et al.* [28] analytically by the Laplace transform technique as shown in Tabs 1 and 2. It has been noted that there is an excellent agreement between the values of the Nusselt number and Sherwood number. This proves the accuracy of the present numerical procedure.

Table 1. Comparison of the Nusselt number N_u when $Q_H = 0$.

P_r	R	γ	t	Abid *et al.* [28]	Present results
0.71	*2*	*1*	*0.2*	*1.3118*	*1.3118*
1.00	*2*	*1*	*0.2*	*1.4661*	*1.4661*
0.71	*4*	*1*	*0.2*	*1.1471*	*1.1471*
0.71	*2*	*2*	*0.2*	*2.0349*	*2.0348*
0.71	*2*	*1*	*0.4*	*1.1056*	*1.1055*

Table 2. Comparison of the Sherwood number S_h when $k_r = 0$.

S_c	t	Abid *et al.* [28]	Present results
0.22	*0.2*	*0.5919*	*0.5919*
0.62	*0.2*	*0.9939*	*0.9940*
0.22	*0.4*	*0.4184*	*0.4185*

4. Results and discussion

In order to evaluate physical significance of the problem due to the effects of the magnetic parameter, permeability parameter, Prandtl number, radiation parameter, heat absorption parameter, Newtonian heating parameter, Schmidt number, chemical reaction parameter, phase angle, time, thermal and mass Grashof numbers on the dimensionless velocity, temperature and concentration, we have computed numerical results and presented them graphically versus η in Figs 1-20 whilst the computed results of the skin friction, Nusselt and Sherwood numbers are put in Tabs 3-6.
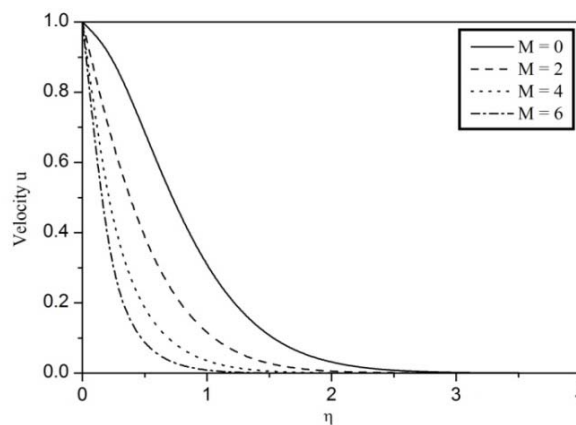

Fig.1. Impact of M on the velocity profiles when $t = 0.1$, $R = 2$, $Q_H = 1$, $P_r = 7$, $S_c = 0.62$, $k_r = 1.0$, $K = 1$, $G_r = 2$, $G_m = 2$, $\gamma = 1$ and $\omega = \pi/4$.

Figure 1 illustrates the effect of the magnetic parameter M on the velocity profiles against η. Physically, $M = 0$ means that there is no magnetic effect and the flow is merely hydrodynamic. The presence of the magnetic field normal to the flow region in an electrically conducting fluid introduces a Lorentz force which works against the flow. Consequently, fluid velocity decreases with an increasing magnetic field

parameter. The influence of the permeability parameter K on the velocity profiles against η is displayed in Fig.2. It is observed that an increase in the permeability parameter tends to accelerate the fluid velocity. Physically, the holes of the porous medium are very large so that the resistance of the medium may be neglected.
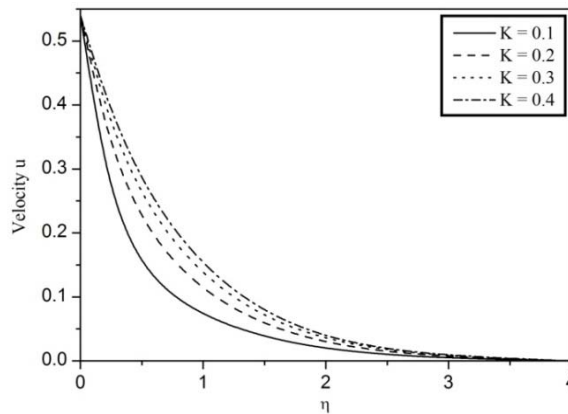

Fig.2. Impact of K on the velocity profiles when $t = 1$, $R = 2$, $Q_H = 0.5$, $P_r = 7$, $S_c = 0.62$, $k_r = 0.5$, $M = 0.5$, $G_r = 3$, $G_m = 2$, $\gamma = 0.5$ and $\omega = \pi/3$.

Figure 3 depicts the variation of velocity profiles against η for four different values of the Prandtl number $P_r = 0.71$, 1, 7 and 100 which correspond to air, electrolytic solution, water and engine oil, respectively. It is clearly seen that the fluid velocity decreases in the boundary layer as the Prandtl number increased. Physically, the fluid with large P_r has high viscosity and small thermal conductivity, which makes the fluid thick and causes a decrease in the fluid velocity in the boundary layer. Also, it is seen that the velocity for air is greater than that of the electrolytic solution, water and engine oil. The variation of velocity profiles against η for different values of the radiation parameter is seen in Fig.4. Physically, $R = 0$ means that there is no radiation only pure convection. It can be seen that the fluid velocity increases with an increasing radiation parameter because large R corresponds to an increased dominance of conduction over radiation thereby increasing the thermal boundary layer thickness.
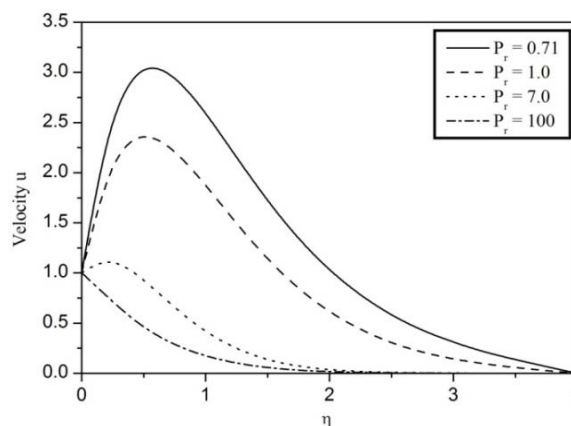

Fig.3. Impact of P_r on the velocity profiles when $t = 0.2$, $R = 2$, $Q_H = 1.0$, $S_c = 0.62$, $k_r = 0.5$, $M = 1.0$, $K = 2$, $G_r = 5$, $G_m = 5$, $\gamma = 1$ and $\omega = \pi/4$.
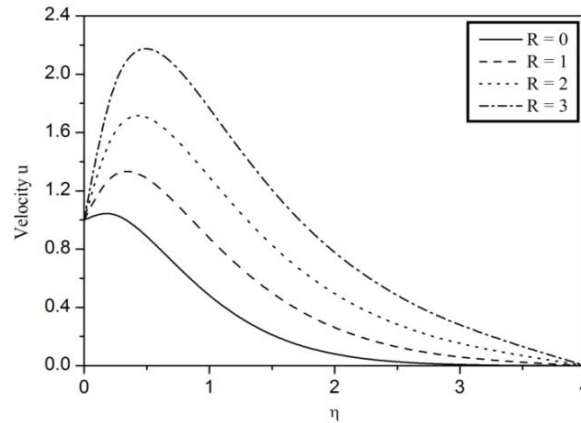
Fig.4. Impact of R on the velocity profiles when $t = 0.2, Q_H = 1.0, P_r = 0.71, S_c = 0.62, k_r = 1.0,$ $M = 2, K = 2, G_r = 5, G_m = 2, \gamma = 1$ and $\omega = \pi/4$.

Figure 5 illustrates the effects of the Newtonian heating parameter γ on the velocity profiles against η. As expected, an increase in γ leads to lessen the fluid density as a result of amplification of the momentum boundary layer thickness. Consequently, an increase in the Newtonian heating parameter tends to increase the fluid velocity. The effect of the Schmidt number S_c on the velocity profiles against η is shown in Fig.6. It is observed that an increase in S_c causes a decline in the fluid velocity due to a decrease in the concentration buoyancy effects. Figure 7 illustrates the effect of the thermal Grashof number G_r on the velocity profiles against η. Physically, G_r represents the effect of free convection current i.e., $G_r = 0$ indicates the absence of free convection currents. It is seen that an increase in G_r tends to enhance the fluid velocity in the boundary layer.
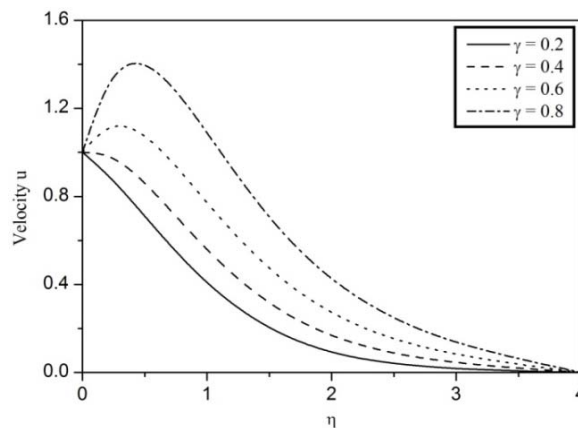

Fig.5. Impact of γ on the velocity profiles when $t = 0.2, R = 3, Q_H = 1, P_r = 0.71, S_c = 0.62, k_r = 0.5, M = 1,$ $K = 2, G_r = 5, G_m = 2$ and $\omega = \pi/4$.
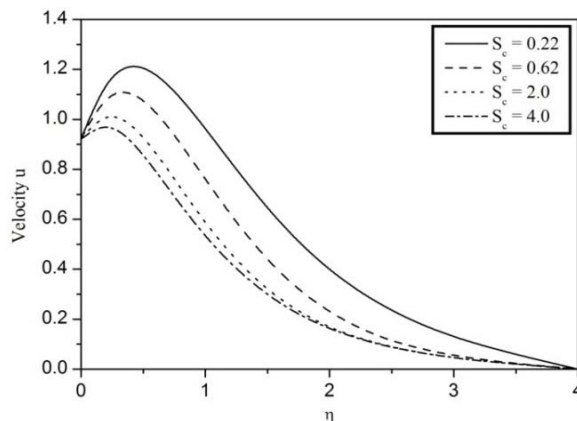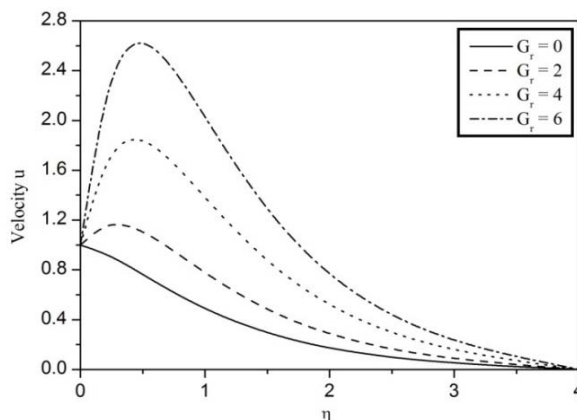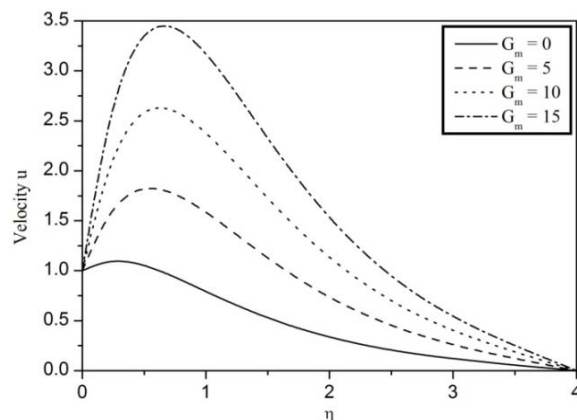
Fig.6. Impact of S_c on the velocity profiles when $t = 0.4$, $R = 2$, $Q_H = 1$, $P_r = 0.71$, $k_r = 0.5$, $M = 0.5$, $K = 2$, $G_r = 5$, $G_m = 3$, $\gamma = 1$ and $\omega = \pi/3$.

Fig.7. Impact of G_r on the velocity profiles when $t = 0.2$, $R = 3$, $Q_H = 1$, $P_r = 0.71$, $S_c = 0.62$, $k_r = 0.5$, $M = 0.5$, $K = 2$, $G_m = 3$, $\gamma = 1$ and $\omega = \pi/4$.

Fig.8. Impact of G_m on the velocity profiles when $t = 0.2$, $R = 3$, $Q_H = 0.5$, $P_r = 0.71$, $S_c = 0.62$, $k_r = 1$, $M = 2$, $K = 1$, $G_r = 4$, $\gamma = 1$ and $\omega = \pi/4$.

The velocity profiles against η for different values of the mass Grashof number G_m are depicted in Fig.8. The effect of G_m on the velocity profiles is same as that of G_r. This is accomplished by comparing Figs.7 and 8. Further, from these figures, we found that velocity suddenly increases near to the plate surface and after this velocity progressively decreases to zero as $\eta \to \infty$. Figure 9 represents the velocity profiles against η for different time. It is clearly seen that the velocity increases with time.
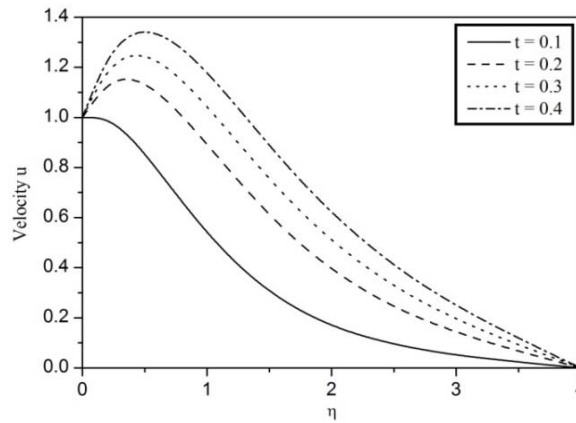

Fig.9. Impact of t on the velocity profiles when $R = 2, Q_H = 1, P_r = 0.71, S_c = 0.62, k_r = 0.5, M = 0.5, K = 2,$ $G_r = 5, G_m = 2, \gamma = 1$ and $\omega = 0$.

The influence of the phase angle ωt on the velocity profiles against η is seen in Fig.10. It is observed that the behavior of the fluid velocity is oscillatory. The velocity is maximum near the plate and decreases with increasing distance from the plate surface and finally approaches zero as $\eta \to \infty$. Also, it is clear from this figure that velocity satisfies the given boundary conditions Eqs.(2.14) and (2.15), which proves the accuracy of our results.
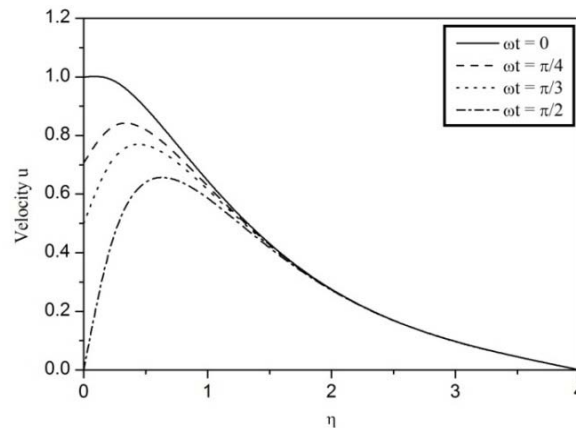

Fig.10. Impact of ωt on the velocity profiles when $t = 1, R = 1, Q_H = 0.5, P_r = 0.71, S_c = 0.22,$ $k_r = 0.5, M = 1, K = 2, G_r = 3, G_m = 2$ and $\gamma = 0.5$.

Further, it has been found that in the absence of heat absorption ($Q_H = 0$) and chemical reaction ($k_r = 0$), the influence of $M, K, P_r, R, \gamma, S_c, G_r, G_m, t$ and ωt on the velocity profiles are quite identical with those (see Figs 2 to 11) of Abid *et al.* [28]. Figure 11 depicts the effect of the heat absorption parameter

Q_H on the velocity profiles against η. It is seen that an increase in the heat absorption parameter decelerates the fluid velocity in the boundary layer. Physically, the presence of heat sink in the boundary layer absorbs energy which causes a decrease in the fluid temperature and as a result decreases the fluid velocity due to the buoyancy effect. The influence of the chemical reaction rate k_r on the velocity profiles against η is seen in Fig.12. It is observed that the fluid velocity decreases with an increasing chemical reaction rate.
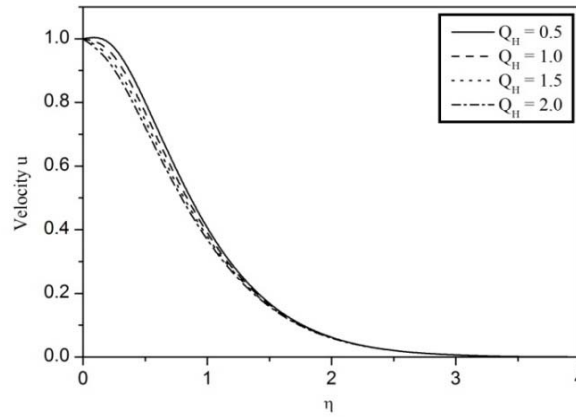

Fig.11. Impact of Q_H on the velocity profiles when $t = 0.2$, $R = 3$, $P_r = 7$, $S_c = 0.62$, $k_r = 1.0$, $M = 2$, $K = 1$, $G_r = 3$, $G_m = 2$, $\gamma = 0.5$ and $\omega = \pi/4$.
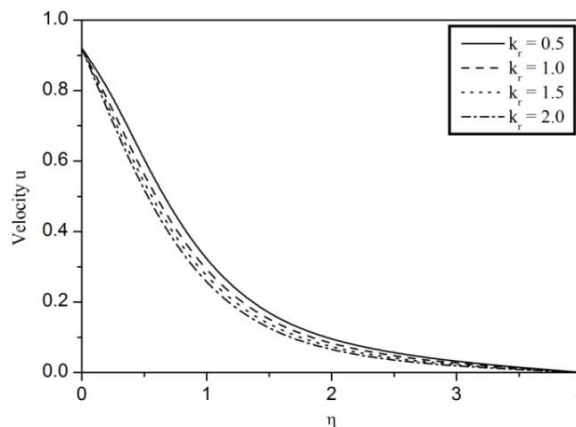

Fig.12. Impact of k_r on the velocity profiles when $t = 0.2$, $R = 3$, $Q_H = 1.0$, $P_r = 7$, $S_c = 0.22$, $M = 2$, $K = 1$, $G_r = 3$, $G_m = 2$, $\gamma = 0.5$ and $\omega = \pi/4$.

Figure 13 exhibits variation of the temperature distribution against η for different values of the Prandtl number P_r. It is observed that an increase in the Prandtl number decreases the fluid temperature due to a decrease of the thermal boundary layer thickness. The influence of the heat absorption parameter Q_H on the temperature distribution against η is seen in Fig.14. It is clear that the fluid temperature decreases with increasing Q_H for the same reason as mentioned above. Figure 15 displays the temperature distribution against η for different values of time t. It is noted that the fluid temperature increases with increasing time. Further, in the absence of radiation $(R = 0)$ and when $\gamma = 1$, the effects of P_r, Q_H and t on the fluid temperature are fairly matching those of Seth *et al*. [29]. This proves the accuracy of the present work.
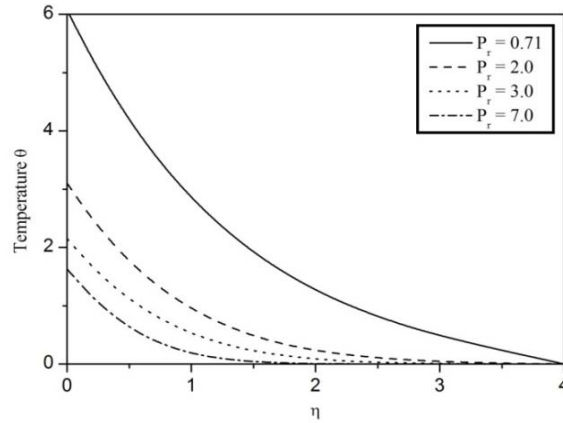
Fig.13. Impact of P_r on the temperature distribution when $t = 0.4$, $R = 3$, $Q_H = 1$ and $\gamma = 1$.

Fig.14. Impact of Q_H on the temperature distribution when $t = 0.2$, $R = 3$, $P_r = 0.71$ and $\gamma = 1$.
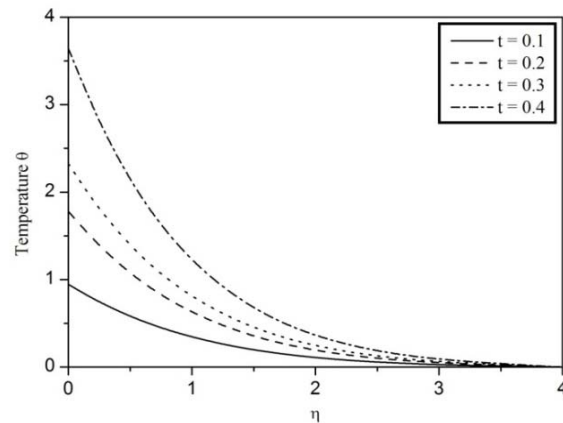
Fig.15. Impact of t on the temperature distribution when $P_r = 0.71$, $R = 1$, $Q_H = 0.5$ and $\gamma = 1$.

The effects of the radiation parameter R on the temperature distribution against η are displayed in Fig.16. An increasing effect is noted in the fluid temperature with increasing radiation parameter for the same reason mentioned above. Figure 17 represents the impact of the Newtonian heating parameter γ on the temperature

distribution against η. We found that an increase in the Newtonian heating parameter enhances the fluid temperature in the boundary layer. Furthermore, it is clear that in the absence of heat absorption ($Q_H = 0$), the effects of P_r, R and t on the temperature distribution are similar to those of Abid *et al.* [28] (see Figs 12 to 15).
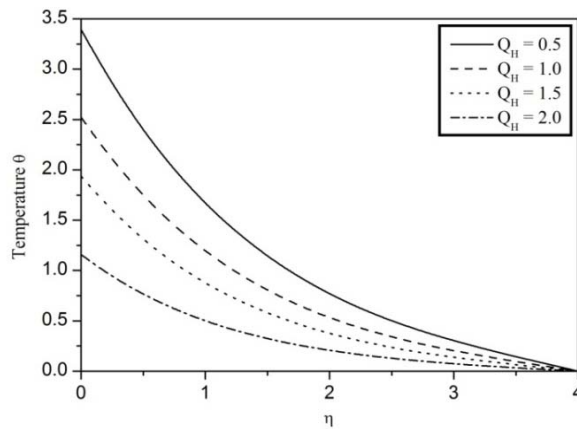

Fig.16. Impact of R on the temperature distribution when $t = 0.2$, $P_r = 0.71$, $Q_H = 0.5$ and $\gamma = 1$.

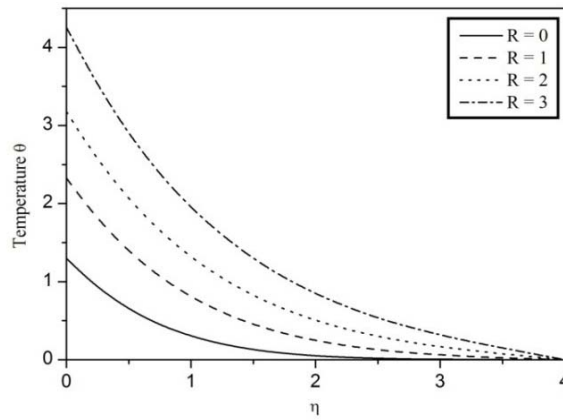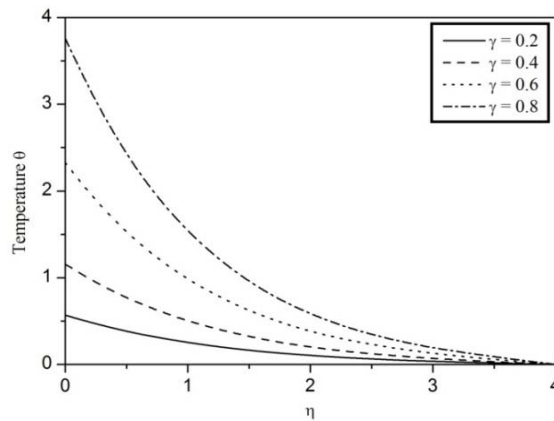Fig.17. Impact of γ on the temperature distribution when $t = 0.2$, $P_r = 0.71$, $R = 3$ and $Q_H = 0.5$.
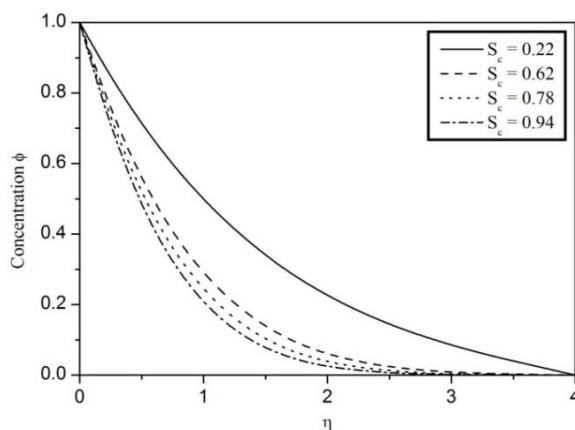

Fig.18. Impact of S_c on the concentration distribution when $t = 0.2$ and $k_r = 1.0$.

Figure 18 is plotted to show the variation of concentration distribution against η for various values of the Schmidt number S_c. It is observed that increasing values of S_c reduce fluid concentration. Physically, an increase of S_c leads to a decrease of molecular diffusivity as a result decreases the concentration boundary layer thickness. The evaluation of concentration distribution against η with time t is displayed in Fig.19.
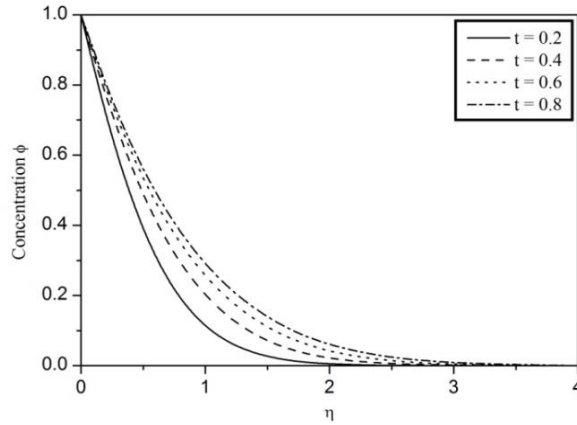
Fig.19. Impact of t on the concentration distribution when $S_c = 0.62$ and $k_r = 0.5$.
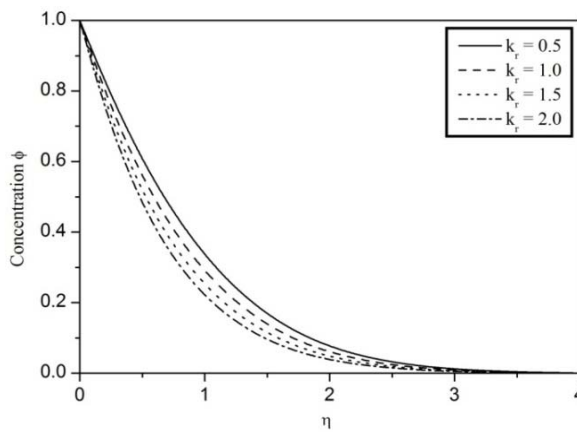
Fig.20. Impact of k_r on the concentration distribution when $t = 0.2$ and $S_c = 0.62$.

Table 3. Comparison of the skin friction τ when . $P_r = 0.71$, $R = 2$, $\gamma = 1$, $S_c = 0.22$, $Q_H = 0$ and $k_r = 0$.

G_r	G_m	M	K	t	ωt	Abid *et al.* [28]	Present results
3	*2*	*0.5*	*0.2*	*0.1*	$\pi/2$	*3.540*	*3.541*
4	*2*	*0.5*	*0.2*	*0.1*	$\pi/2$	*4.072*	*4.075*
3	*3*	*0.5*	*0.2*	*0.1*	$\pi/2$	*3.221*	*3.220*
3	*2*	*1.0*	*0.2*	*0.1*	$\pi/2$	*3.609*	*3.610*
3	*2*	*0.5*	*0.4*	*0.1*	$\pi/2$	*3.297*	*3.297*
3	*2*	*0.5*	*0.2*	*0.2*	$\pi/2$	*0.621*	*0.626*
3	*2*	*0.5*	*0.2*	*0.1*	π	*3.349*	*3.349*

It can be seen that the fluid concentration increases with increasing time. Moreover, this figure verifies the concentration boundary condition given in Eqs. (2.14) and (2.15). Initially, concentration takes the value 1 and soon after for large values of $\eta(\eta > 0)$ it tends to zero with an increase of t. Furthermore, it is noted that in the absence of the chemical reaction rate $(k_r = 0)$ the effects of S_c and t on the concentration distribution are same as those (see Figs 16 and 17) in Abid *et al.* [28]. The variation of concentration distribution against η for various values of the chemical reaction rate k_r is depicted in Fig.20. It is observed that an increase in k_r reduces the concentration of species in the boundary layer.

The computed numerical results of the skin friction coefficient, Nusselt number and Sherwood number are displayed in Tabs 3-6 for different values of key parameters. It is observed from Tabs 3 and 4 that the skin friction improves with an increase in G_r, P_r, M and k_r whilst a reverse tendency is noted with an increase in G_m, K, t, ωt, R, γ, S_c and Q_H. These tables show an excellent agreement between the numerical values of the skin friction coefficient in the present study and past work of Abid *et al.* [28] in the absence of the heat absorption parameter $(Q_H = 0)$ and chemical reaction rate $(k_r = 0)$. It is seen from Tab.5 that the Nusselt number increases with increasing P_r, γ and Q_H whilst it decreases with increasing R and t. An increase in S_c and k_r increases the Sherwood number whilst a reverse effect is observed when t is increased as seen in Tab.6.

Table 4. Comparison of the skin friction τ when $G_r = 3$, $G_m = 2$, $M = 0.5$, $K = 0.2$, $t = 0.1$ and $\omega t = \pi/2$.

P_r	R	γ	S_c	Q_H	k_r	Abid *et al.* [28]	Present results
0.71	2	1.0	0.22	0.0	0.0	3.540	3.541
1.0	2	1.0	0.22	0.0	0.0	5.251	5.250
0.71	3	1.0	0.22	0.0	0.0	2.413	2.413
0.71	2	1.5	0.22	0.0	0.0	0.915	0.917
0.71	2	1.0	0.62	0.0	0.0	3.467	3.467
0.71	2	1.0	0.22	1.0	0.5	---	3.256
0.71	2	1.0	0.22	1.5	0.5	---	2.642
0.71	2	1.0	0.22	1.0	1.0	---	3.583

Table 5. Numerical values of the Nusselt number N_u.

P_r	R	γ	Q_H	t	N_u
0.71	2	1	1.0	0.2	1.1342
7.00	2	1	1.0	0.2	2.1649
0.71	3	1	1.0	0.2	1.0375
0.71	2	2	1.0	0.2	2.5792
0.71	2	1	1.5	0.2	1.6031
0.71	2	1	1.0	0.4	0.9681

Table 6. Numerical values of the Sherwood number S_h.

S_c	t	k_r	S_h
0.22	0.2	0.5	0.7041
0.62	0.2	0.5	1.2151
0.22	0.4	0.5	0.5169
0.22	0.2	1.0	0.8273

5. Conclusions

The effect of Newtonian heating on a heat absorbing unsteady MHD free convective flow past an oscillating vertical porous plate embedded in a porous medium in the presence of thermal radiation and chemical reaction has been studied numerically by the finite element method. The following major conclusions have been drawn from the present study:

−   The fluid velocity increases with an increase in R, γ, t, K, G_r and G_m, whereas it decreases with an increase in P_r, S_c, M, Q_H, k_r and ωt.

− P_r and Q_H have a tendency to decrease in the temperature distribution, whereas R, γ and t show an opposite tendency.

−   There is a decrease in the concentration distribution with an increase in S_c or k_r, whereas a reverse trend is noticed when t is increased.

−   The value of the skin friction coefficient improves with an increase in G_r, P_r, M and k_r, whereas it decreases with an increase in $G_m, K, R, \gamma, S_c, Q_H, \omega t$ and t.

−   Increasing value of P_r, Q_H and γ increases the Nusselt number, whereas it decreases with an increase in R and t.

−   The value of the Sherwood number increases with an increase in S_c or k_r, whereas it decreases with an increase in t.

Nomenclature

B_0 – magnetic induction $\left(Am^{-1} \right)$

C' – species concentration $\left(\mathrm{mol}\, m^{-3} \right)$

C_p – specific heat $\left(Jkg^{-1}k \right)$

C'_w – plate surface concentration $\left(\mathrm{mol}\, m^{-3} \right)$

C'_∞ – free stream concentration $\left(\mathrm{mol}\, m^{-3} \right)$

D – mass diffusivity $\left(m^2 s^{-1} \right)$

g – acceleration due to gravity $\left(ms^{-2} \right)$

G_m – mass Grashof number

G_r – thermal Grashof number

K – permeability parameter

k – thermal conductivity $\left(Wm^{-1}K^{-1} \right)$

k_r' – reaction coefficient

M^2 – magnetic field parameter

N_u – Nusselt number

P_r – Prandtl number

Q_0' – heat absorption coefficient

Q_H – heat absorption parameter

q_r – radiation heat flux $\left(W/m^2\right)$

R – radiation parameter

S_h – Sherwood number

S_c – Schmidt number

T' – fluid temperature (K)

t' – time (s)

T_∞' – free stream temperature (K)

x' – co-ordinate axis along the plate (m)

y' – co-ordinate axis normal to the plate (m)

u – dimensionless velocity $\left(ms^{-1}\right)$

u' – fluid velocity $\left(ms^{-1}\right)$

U_0 – amplitude of the plate oscillations

β – volumetric coefficient of thermal expansion $\left(K^{-1}\right)$

β^* – volumetric coefficient of concentration expansion $\left(K^{-1}\right)$

η – dimensionless variable

θ – dimensionless temperature

ν – kinematic viscosity $\left(m^2 s^{-1}\right)$

μ – dynamic viscosity $\left(Kg/m^{-1}s^{-1}\right)$

ρ – fluid density $\left(Kg/m^3\right)$

σ – electrical conductivity (S/m)

ϕ – dimensionless concentration

τ – skin friction coefficient $\left(Nm^{-2}\right)$

ω – frequency of oscillations

References

[1] Das U.N., Deka R.K. and Soundalgekar V.M. (1994): *Effects of mass transfer on flow past an impulsively started infinite vertical plate with constant heat flux and chemical reaction.* – Forschung im Ingenieurwesen, vol.60, pp.284-287.

[2] Muthucumaraswamy R. and Ganesan P. (2001): *First order chemical reaction on flow past an impulsively started vertical plate with uniform heat and mass flux.* – Acta Mechanica, vol.147, pp.45-57.

[3] Raptis A. and Perdikis C. (2006): *Viscous flow over a non-linearly stretching sheet in the presence of chemical reaction and magnetic field.* – International Journal of Non-Linear Mechanics, vol.41, pp.527-529.

[4]   Cortell R. (2007): *MHD flow and mass transfer of an electrically conducting fluid of second grade in a porous medium over stretching sheet with chemically reactive species.* − Chemical Engineering Process, vol.46, pp.721-728.

[5]   Muthucumaraswamy R. and Janakiraman B. (2008): *Mass transfer effects on isothermal vertical oscillating plate in the presence of chemical reaction.* − International Journal of Applied Mathematics and Mechanics, vol.4, No.1, pp.66-74.

[6]   Mahapatra N., Dash G. C., Panda S. and Acharya M. (2010): *Effects of chemical reaction on free convection flow through a porous medium bounded by a vertical surface* − Journal of Engineering Physics and Thermo-Physics, vol.83, No.1, pp.130-140.

[7]   Rajesh V. and Varma S.V.K. (2010): *Chemical reaction effects on free convection flow past an exponentially accelerated vertical plate* − Annals Journal of Engineering, VIII, Fascicule, No.1, pp.181-188.

[8]   Rajesh V. (2010): *MHD and chemical reaction effects on free convection flow with variable temperature and mass diffusion* − Annals Journal of Engineering, VIII, Fascicule, No.3, pp.370-378.

[9]   El-Fayez F.M.N. (2012): *Effects of chemical reaction on the unsteady free convection flow past an infinite vertical permeable moving plate with variable temperature* − Journal of Surface Engineered Materials and Advanced Technology, vol.2, pp.100-109.

[10] Sehkar D.V. and Reddy G. V. (2012): *Effects of chemical reaction on MHD free convective oscillatory flow past a porous plate with viscous dissipation and heat sink.* − Advances in Applied Science Research, vol.3, No.5, pp.3206-3215.

[11] Soundalgekhar V.M. and Takhar H.S. (1993): *Radiation effects on free convection flow past a semi-infinite vertical plate.* − Modeling Measurement and Control, vol.B, No.51, pp.31-40.

[12] Takhar H.S. Gorla R.S. and Soundalgekhar V.M. (1996): *Radiation effects on MHD free convection flow of a radiating gas past a semi-infinite vertical plate.* − International Journal of Numerical Methods for Heat and Fluid Flow, vol.6, No.2, pp.77-83.

[13] Raptis A. and Perdikis C. (1999): *Radiation and free convection flow past a moving plate.* − Applied Mechanics and Engineering, vol.4, No.4, pp.817-821.

[14] Chamkha A.J., Takhar H.S. and Beg O. (2004): *Radiative free convective non-Newtonian fluid flow past a wedge embedded in a porous medium.* − International Journal of Fluid Mechanics Research, vol.31, No.2, pp.101-115.

[15] Muthucumaraswamy R. and Janakiraman B. (2006): *MHD and radiation effects on moving isothermal vertical plate with variable mass diffusion.* − Theoretical Applied Mechanics, vol.33, No.1, pp.17-29.

[16] Rajesh V. and Varma S.V.K. (2010): *Radiation effects on MHD flow through a porous medium with variable temperature and mass diffusion.* − International Journal Applied Mathematics and Mechanics, vol.6, No.1, pp. 39-57.

[17] Mebine P. and Adigio E.M. (2011): *Effects of thermal radiation on transient MHD free convection flow over a vertical surface embedded in a porous medium with periodic boundary conditions.* − Mathematica Aeterna, vol.I, pp.245-261.

[18] Sharma S. and Deka R.K. (2012): *Thermal radiation and oscillating temperature effects on unsteady MHD flow past a semi infinite porous vertical plate in the presence of chemical reaction.* − International Journal of Physics and Mathematical Sciences, vol.2, No.2, pp.33-52.

[19] Muralidhran M. and Muthucumaraswamy R. (2013): *Radiation effects on linearly accelerated plate with variable mass diffusion in the presence of magnetic field.* − Applied Mathematical Sciences, vol.7, No.113, pp.5645-5656.

[20] Merkin J.H. (1994): *Natural convection boundary layer flow on a vertical surface with Newtonian heating.* − International Journal for Heat and Fluid Flow, vol.15, pp.392-398.

[21] Lesnic D., Ingham D.B. and Pop I. (1999): *Free convection boundary layer flow along a vertical surface in a porous medium with Newtonian heating.* − International Journal of Heat and Mass Transfer, vol.42, pp.2621-2627.

[22] Lesnic D., Ingham, D.B. and Pop I. (2000): *Free convection flow from a horizontal surface in a porous medium with Newtonian heating.* − Journal of Porous Media, vol.3, pp.227-235.

[23] Lesnic D., Ingham D.B., Pop I. and Storr C. (2004): *Free convection boundary layer flow above a nearly horizontal surface in a porous medium with Newtonian heating.* − Heat Mass Transfer, vol.40, pp.665-672.

[24] Chaudhary R.C. and Jain P. (2006): *Unsteady free convection boundary layer flow past an impulsively started vertical plate with Newtonian heating.* − Rom Journal of Physics, vol.51, pp.911-925.

[25] Salleh M.Z., Nazar R. and Pop I. (2009): *Forced convection boundary layer flow at a forward stagnation point with Newtonian heating.* − Chemical Engineering Communication, vol.196, pp.987-996.

[26] Salleh M.Z., Nazar R. and Pop I. (2010): *Boundary layer flow and heat transfer over a stretching sheet with Newtonian heating.* – Journal of Taiwan Institute of Chemical Engineers, vol.41, pp.651-655.

[27] Abid H., Khan I. and Shafi S. (2013): *An exact analysis of heat and mass transfer past a vertical plate with Newtonian heating.* – Journal of Applied Mathematics, Article ID: 434571, pp.1-9.

[28] Abid H., Ismail Z., Khan I., Hussein A.G. and Shafi S. (2014): *Unsteady boundary layer MHD free convection flow in a porous medium with constant mass diffusion and Newtonian heating.* – European Physical Journal Plus, vol.129, No.46, p.16, DOI 10.1140/epjp/i2014-14046-x.

[29] Seth G.S., Sarkar S. and Nandkeolyar R. (2015): *Unsteady hydro-magnetic natural convection flow past an impulsively moving vertical plate with Newtonian heating in a rotating system.* – International Journal of Applied Fluid Mechanics, vol.8, No.3, pp.623-633.

[30] Magyari E. and Pantokratoras A. (2011): *Note on the effect of thermal radiation in the linearized Rosseland approximation on the heat transfer characteristics of various boundary layer flows.* – International Communication Heat and Mass Transfer, vol.38, pp.554-556.

[31] Reddy J.N. (1985): *An Introduction to the Finite Element Method.* – McGraw-Hill, New York.

[32] Bathe K.J. (1996): *Finite Element Procedures.* – Prentice-Hall, New Jersey.